

## Fractal Dimension as Robust Estimate of Low Carbon Steels Hardness

Krzysztof Zajac<sup>1</sup>, Karolina Płatek<sup>2</sup>, Paweł Wachel<sup>3</sup>, Leszek Łatka<sup>2\*</sup>

<sup>1</sup> Faculty of Microsystem Electronics and Photonics, Wrocław University of Science and Technology, ul. Janiszewskiego 11, 50-372 Wrocław, Poland

<sup>2</sup> Faculty of Mechanical Engineering, Wrocław University of Science and Technology, ul. Łukasiewicza 5, 50-371 Wrocław, Poland

<sup>3</sup> Faculty of Information and Communication Technology, Wrocław University of Science and Technology, ul. Janiszewskiego 11, 50-372 Wrocław, Poland

\* Corresponding author's e-mail: [leszek.latka@pwr.edu.pl](mailto:leszek.latka@pwr.edu.pl)

### ABSTRACT

Application of computational methods in engineering and science constantly increases, which is also visible in sector of material science, often with promising results. In following paper, authors would like to propose fractal dimension, a mathematical method of quantifying self-similarity and complexity of spatial patterns, as robust method of hardness estimation of low carbon steels. A dataset of microstructure images and corresponding Vickers hardness measurements of S235JR steel under different delivery conditions was created. Then, three different computational methods for evaluation of materials hardness based on microstructure image were tested. In this paper those methods are called: (i) Otsu-based index, (ii) fractal dimension index and (iii) vision transformer index. The results were compared with method used in literature for similar problems. Comparison showed that fractal dimension performs better than other evaluated methods, in terms of median absolute error, which value was equal to 4.12 HV1, which is significantly lower than results achieved by Otsu-based index and vision transformer index, which were 4.49 HV1 and 5.07 HV1 respectively. Those results can be attributed to the relative robustness of fractal dimension index, when compared to other methods. Robust estimation is preferable, due to the high amount of noise in the dataset, which is a consequence of the nature of used material.

**Keywords:** fractal dimension, linear regression, robust hardness estimation, image processing, low carbon steels

### INTRODUCTION

Hardness, defined as the ability of a material to resist deformation, is one of the most important materials' properties. Its value is associated with abrasion wear resistance or cavitation erosion resistance [1, 2]. Moreover, correlation between hardness and tensile strength was also proven [3, 4].

For measuring materials' hardness, different methods are used, depending on properties of tested material, or required results of the test. For metallic materials, Vickers method is often applied due to its universality as this method can be used for versatile materials and covers wide hardness

range. In this method, a diamond indenter with a shape of square-based pyramid is pressed against the surface of tested specimen with a certain load. The value of a load depends on expected properties of tested material. Hardness of tested specimen is based on length of diagonal of the mark left in material. The whole procedure is precisely described in ISO 6507 standard [5]. Hardness can also be determined with scratching tests, for example the Bierbaum scratch test or Mohs hardness test, or by measuring recovery efficiency or resilience, such as Rockwell test [6].

Application of computational methods in engineering and material science constantly increases. Majority of works are considering

application of computational methods for analyzing, designing, simulating, or controlling physical phenomena [7, 8]. Computational methods such as machine learning algorithms were successfully applied to material science, both to design and examine materials structure [9, 10]. In [11] authors presented an interesting attempt in using artificial intelligence techniques to characterize the microstructure of a Ni-based alloy base on ultrasound signals. Bayesian approach was also presented by Jung et al. [12] and adapted to predict mechanical properties of dual-phase steels in [13].

Computer vision methods can be divided into two broad categories: those based on digital image processing techniques together with statistical methods and those based on deep learning models, often utilizing end to end training procedures. First category usually consists of two steps: feature extraction, which quantifies information in digital image into numerical values and statistical algorithm, estimating desired target values based on those features. Such methods have been successfully applied in material science [14, 15], including hardness estimation from microstructure images [16, 17].

Robust statistics is used for problems with high presence of noise, to reduce its influence on estimated quantities. Even in case of carbon steels, the influence of alloying elements, especially manganese, on materials hardness is non-negligible. In such case robustness of statistical tools is essential for meaningful predictions. The field of robust statistics contains numerous methods for outlier-robust regression [18, 19], and theory suggests that learning algorithms with smaller number of variables are preferred, since they have smaller statistical variance, which in turn results in smaller influence of the noise in the dataset.

In this paper, we propose fractal dimension as robust method of hardness estimation of low carbon steels. Fractal dimension is a mathematical concept used for quantifying self-similarity and complexity of spatial patterns [20]. This leads to a hypothesis that it should provide a robust estimate of material hardness, based on the microstructure image, since in a single number it quantifies the complexity and space-filling properties of the considered image. Fractal dimension has been

successfully used in problems from the domain of computer vision, for example facial recognition [21] and many others [22]. Fractal analysis is already broadly used in material science and its main fields of application include geometrical characteristics of the surface, grain size and materials porosity [23–25]. Moreover, some attempts for implementation of fractal dimension in microstructure analysis were also made [26]. In [27], a direct correlation between fractal dimension of fracture surface and fatigue loading was successfully established.

## DATA ACQUISITION

### Materials

The following research was focused on low-carbon structural steels, due to their wide spectrum of industrial applications and low content of alloying elements. According to [28] standard, low-carbon steel should contain no more than 0.3 wt% of carbon. Its structure is nonhomogeneous and contains primarily ferrite with fractions of pearlite. For this purpose, low-carbon S235JR (according to standard [29]) structural steel, was chosen. S235JR is widely used in industrial applications mainly because of its excellent weldability and machineability. Its applications include industrial pipes or civil engineering [30]. Chemical composition of S235JR steel is presented in Table 1 in accordance with [31] standard. Due to impact of delivery conditions on materials' properties, authors decided to examine chosen material in two condition states: hot-rolled and normalized.

### Sample preparation and measurement process

Each sample was grinded and polished using diamond suspension. Etching was performed using 3% Nital solution [32]. Images of the microstructure were taken using optical microscope Keyence VX6000. The magnification was equal to 400x. All images were divided into four sections of equal size and for each section, one hardness measurement was taken, as presented in

**Table 1.** Chemical composition of S235JR steel according to EN 10025 standard, wt% [31].

C	Mn	P	S	N	Cu	Fe
0.17	1.40	0.035	0.035	0.12	0.55	Balance

Figure 1. Hardness was measured using Vickers Test method, in accordance with [5] standard, with a maximum test force equal to 9.81 N (HV1).

### Measurements results

As a result of microscopic observations, a dataset of 288 microstructure images was created with 1139 corresponding measurements. The number of measurements is slightly lower than 1152, since some of them had to be removed due to errors that occurred during Vickers hardness test. Microscopic observations showed that microstructure of all examined samples corresponds with presumed requirements. No influential defects were noticed. Exemplary images of microstructure are shown in Figure 2. Visibly textured pearlite fractions of hot-rolled steel in comparison with normalized one are a result of its delivery condition. Average measured hardness of

normalized S235JR steel was 136 HV1 with a standard deviation of 9.9 HV1, while hot-rolled one exhibits slightly higher average value ( $139 \text{ HV1} \pm 7.1 \text{ HV1}$ ) what is also related to its delivery conditions. Hardness values distribution is shown in Figure 3. Total number of measurements of normalized and rolled S235JR steel were 495 and 644 respectively.

### Sampling

Each material sample consists of four independent measurements, each with a corresponding region of the image, as presented in Figure 1. Significantly outlying measurements from the dataset were removed, by computing maximal distance from the mean, inside a single material sample, with a cut-off value of 15 HV1. The formula for computing this deviation is given in Equation 1, where  $\bar{x}$  denotes the mean value of all

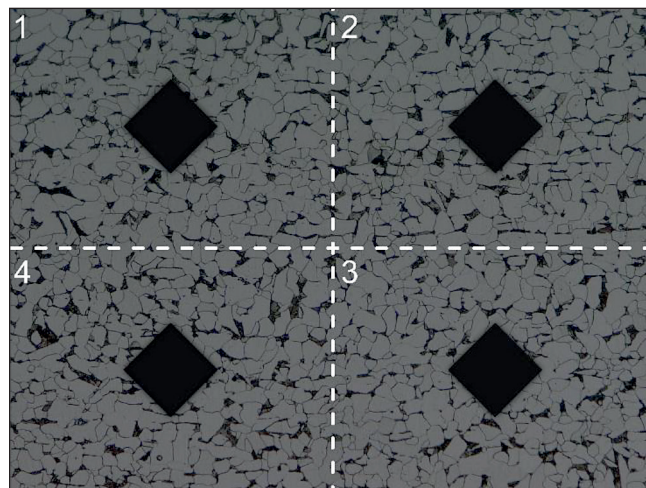


**Figure 1:** Representation of microstructure image with hardness measurements marks visualised.

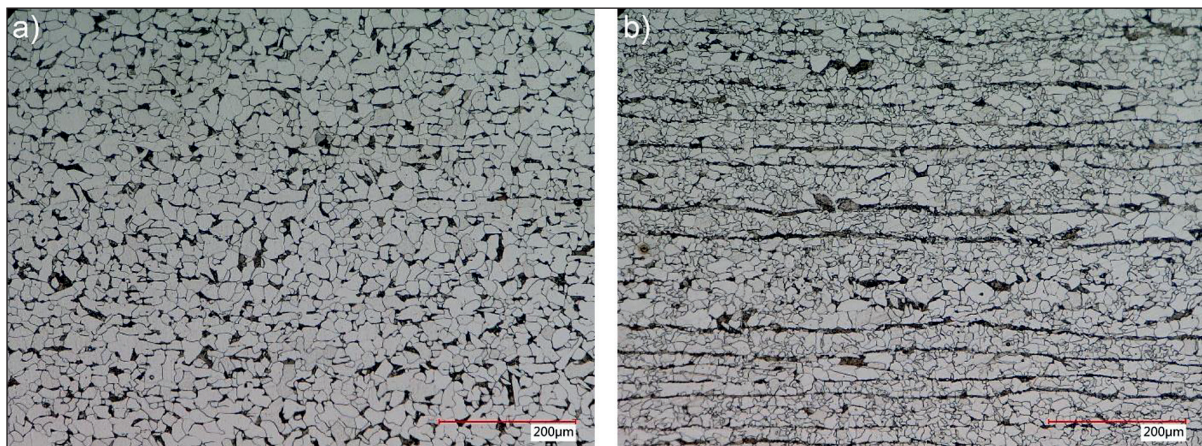


**Figure 2:** Exemplary images of different textures presented by S235JR steel: a) texture pattern is slightly visible due to normalization; b) demonstrably textured microstructure as a result of hot-rolling process.

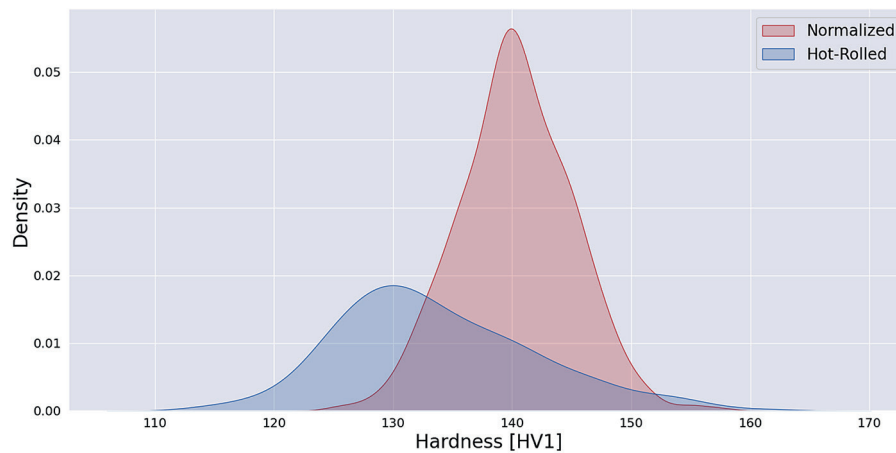


**Figure 3:** Comparison of hardness values distribution of S235JR steel at different delivery conditio

measurements corresponding to a single sample. Dataset was further split into the train and test, with ratio of 70 to 30%. To prevent information leakage into the test dataset, we draw entire samples, with four measurements and images into the test set, however we do not account for the steel type. This results in train dataset with 399 hot-rolled samples and 203 normalized samples and a test dataset with 140 hot-rolled samples and 116 normalized samples.

$$\max(|x - \bar{x}|) \tag{1}$$

### HARDNESS ESTIMATION METHODS

A set of three methods of hardness estimation is proposed with varying number of parameters: Otsu-based index, fractal dimension index and vision transformer index. Otsu-based index and fractal dimension index are based on image processing methods and linear regression, both having a small number of trainable parameters, while vision transformer index is a deep learning method, which utilizes transfer learning paradigm [33] to generate abstract numerical representation of each image, which is passed to a shallow neural network. This method has significantly greater number of trainable parameters than Otsu-based index and fractal dimension index.

#### Otsu-based index

Otsu based index is a method using automatic image thresholding to extract features from the microstructure image [34]. Firstly,

image is converted to grayscale since Otsu’s method only works with single channel images. Then it is converted to binary image using estimated Otsu threshold. This binary representation is converted to numerical features by simply counting the ratio of dark and bright pixels, which results in two values representing each image. Those values are then passed to linear regression model, used as the estimate of hardness.

#### Vision transformer index

Vision transformer index, as a method proposed in this study uses transfer learning (for a vision transformer deep learning model) to estimate hardness of microstructure images. Transfer learning is a technique commonly used in machine learning, particularly often with deep learning models with a high number of parameters. Those models are trained on one task, but their parameters are next transferred to a different task, usually changing last few layers of the neural network. Those steps are commonly called pre-training and fine-tuning. Usually, during fine-tuning most of the parameters are frozen, which makes the computation of gradient required to train the model easier. This approach is possible, due to high representational abilities of large neural networks, which are able to generate abstract representations of input data and it has been successfully used in numerous settings, including computer vision [35, 36] and natural language processing [37].

Vision transformer is a deep learning model designed for image processing [38], which

modifies transformer architecture [39] originally designed for natural language processing, to process images. It is particularly well-suited for transfer learning. For the purpose of this experiment other deep learning models were used as basis for hardness estimation, including ResNet family [40], but vision transformer model achieved best performance, hence this method was pre-selected for further studies and called vision transformer index. In this case model was trained on large dataset for image classification, called ImageNet 21k [41], models pre-trained on different datasets are also available.

Vision transformer index computation consists of two neural networks (although they can be conceptually treated as one). Firstly, image is converted to an abstract numerical representation, called embedding, which is processed by another, shallow network to predict hardness of the corresponding input image. This is described by formulae from Equation 2 and Equation 3, where  $H$  denotes hidden vector of representation generated by vision transformer, with 768 dimensions and  $\hat{h}$  denotes estimated hardness.  $VIT$  and  $NN$  denote vision transformer and fully trainable neural network respectively.

$$H = VIT(x) \tag{2}$$

$$\hat{h} = NN(H) \tag{3}$$

### Fractal dimension index

The concept of fractal dimension was introduced by B. Mandelbrot [20] as a generalization of the integer dimensionality of space/object. Informally, integer dimensions have a property, that when an object is scaled by a coefficient, denoted as  $1/r$ , its measure would change, following formula given by Equation 4.

$$N = r^D \tag{4}$$

where:  $D$  is this object's dimension.

This leads to a generalization, for irregular objects, different than straight lines or planes, to non-integer dimension. After transforming formula from Equation 4, the fractal dimension can be derived as follows in Equation 5.

$$D = \frac{\log(N)}{\log(r)} \tag{5}$$

This value can be assigned to any shape, including images, after they are converted to binary form. All possible binary images, except those with only single value, would have a fractal dimension between 1 and 2. To compute fractal dimension index, image is converted to binary, using Canny edge filter [42]. Later fractal dimension is computed using box-counting dimension, also called Minkowski – Bouligand dimension [43]. The formula for computing box-counting dimension is given by Equation 6.

$$D_{BC} = \lim_{r \rightarrow 0} \frac{\log N(r)}{\log(1/r)} + 2 \tag{6}$$

Box-counting in images is implemented by counting the number of dark pixels covered by boxes of increasing size, starting from box with size of a single pixel. Using formula from Equation 6 the dimension is estimated as a slope of computed values, using numerical method of fitting slope coefficient to linear equation based on computed box counts. This dimension is computed for all images and its values are passed to a linear regression model, which learns the relation between them and measured hardness. Figure 4 and Figure 5 show processed microstructures, with highest and lowest values of fractal dimension in the training dataset of 1.84 and 1.71 respectively. Computed hardness values using the fitted linear regression were equal to 144 HV1 and 129 HV1.

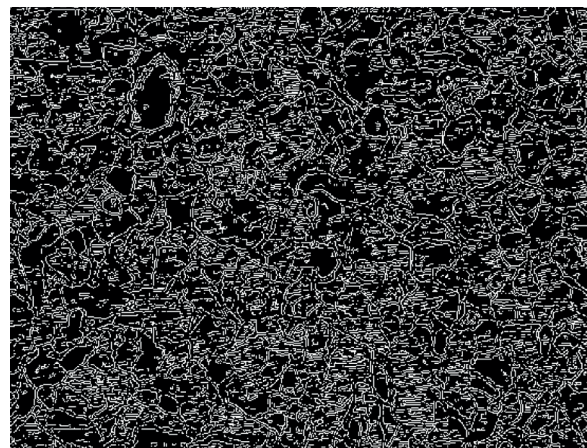
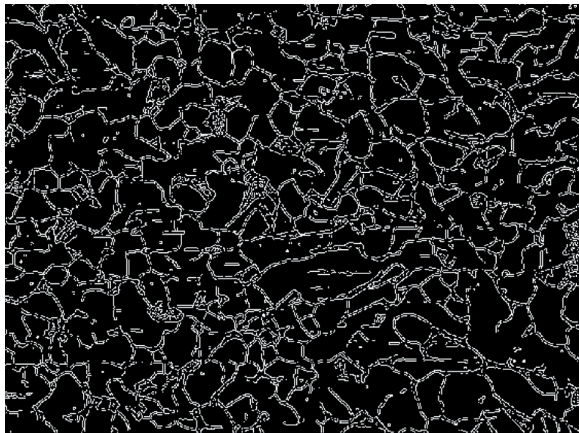


Figure 4: Processed microstructure with computed fractal dimension of 1.84.



**Figure 5:** Processed microstructure with computed fractal dimension of 1.71.

## EVALUATION METRICS

Reported metrics are Mean Absolute Error (MAE), Median Absolute Error (MDE) and Standard Deviation of model predictions (STD). Additionally, we include a number of learnable parameters of the predicting models (#P). This value does not include tuneable hyperparameters, for example the standard deviation of the Gaussian filter used in Canny detector of fractal dimension index. Those metrics are selected, since they are most suitable to evaluate problems with high amount of noise in the dataset. Often considered factor  $R^2$  is not included, since hardness distribution has relatively small standard deviation, which causes the values of this metric to be uninformative.

## Experiments

All models described in Section 3 were evaluated on the test set of microstructure images and hardness measurements. Only the best results from each model are reported, since numerous runs were conducted for each of them with varying hyperparameters. Additionally, baseline model and linear regression model based on 2-point correlation and principal component analysis is

included for comparison, following the implementation described by Nikhil et.al [16], further called simply 2-point correlation. Baseline model is not learnable, and simply returns mean hardness of training set for all images. All models were trained using transformed values of hardness, using mean substitution and division by the standard deviation. Reported metrics are computed using inversely transformed predictions, back to the original measured range.

## RESULTS

Table 2 shows metrics evaluated for different models. Fractal dimension index has smallest errors, both in terms of mean and median. For mean baseline the number of parameters (#P), is equal to 1, since it only stores the mean hardness of the training set. For Otsu-based index, fractal dimension index and 2-point correlation, #P's are the numbers of learnable parameters in linear regression. Finally, for a vision transformer index, #P is the number of all learnable parameters of the predicting part of the model. Results are discussed in Conclusions section.

### Fractal dimension index analysis

One of the hyperparameters of fractal dimension index method is standard deviation of Gaussian filter used in Canny detector. It has significant influence on computation of the fractal dimension and leads to changes in performance of the model. Figure 6 shows the dependency of this value on median absolute error. All further results are using the optimal found value, equal to 0.8.

In statistical modelling, it is sometimes useful to generate new features for the model to make it learn more complex dependencies. In case of fractal dimension index, regression model has just one input variable, so it could be beneficial to create more features. This is achieved by generating higher powers of the fractal dimensions, up

**Table 2:** Metrics evaluated for different models

Method	#P	MAE	MDE	STD
Mean baseline	1	6.44	5.36	0.00
Otsu-based index	3	5.64	4.49	3.20
Fractal dimension index	2	5.16	4.12	3.83
2-point correlation	21	5.73	4.90	2.90
Vision transformer index	30801	5.74	5.07	5.65

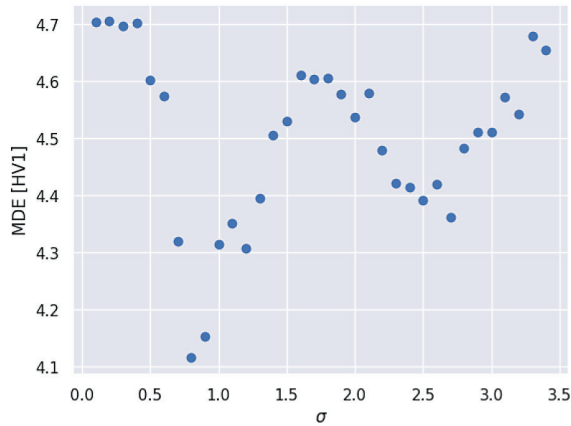


**Figure 6.** Dependency of fractal dimension value on median absolute error

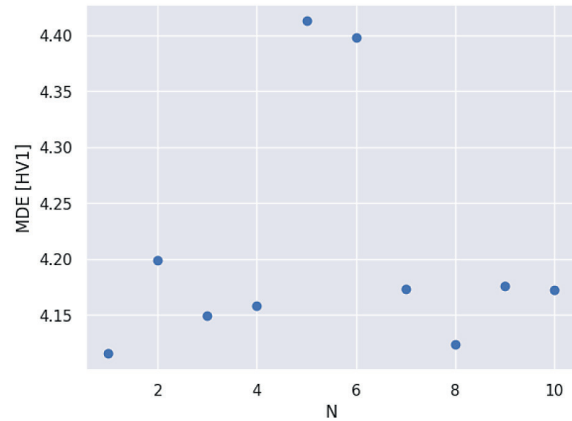


**Figure 7.** Dependency of fractal dimension value on median absolute error for fractal dimensions

to tenth. The results are presented in Figure 7. No significant benefit was observed for dataset used in the experiment. For non-optimal values of sigma, different than 0.8, it is possible to observe improvement by adding those higher order powers of fractal dimension, however no model achieved better performance than using just the first power of fractal dimension, when it was computed using optimal sigma value in the Canny filter.

Additionally different downstream models were evaluated, other than linear regression. The results are presented in Table 3. No improvement over the linear regression-based index was observed, which supports the hypothesis, that dataset used in the experiment requires robust approach, with low statistical variance. Evaluated models, other than linear regression were: Gaussian processes based regression [44], support vector machine [45, 46] and multi layered perceptron [47]. Figure 8 shows the learned dependency, between fractal dimension and material hardness, with all examples of the test dataset.

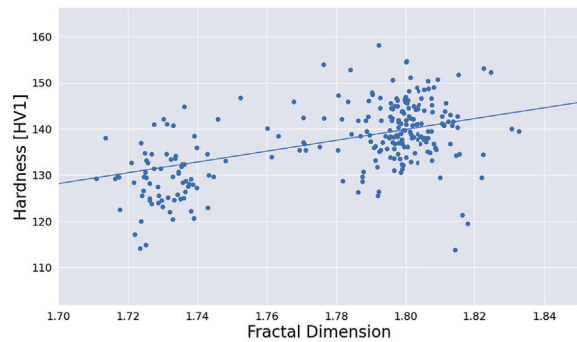


**Figure 8.** Learned dependency between fractal dimension and material hardness for linear regression

## CONCLUSIONS

To conclude, we have developed a computational method for hardness evaluation from microstructure images based on fractal dimension

analysis. The dataset containing 1139 hardness measurements and corresponding images of S235JR steel was used for this case. Result of this study may potentially lead to development in techniques used for microstructure image analysis. Moreover, correlation between materials properties and its fractal dimension might become useful tool in both examination and tailoring materials properties. However, further research is required. Following conclusions were drawn from the results of conducted experiments.

- Fractal dimension is potentially robust feature, which can be used for prediction of materials' properties using microstructure images. However, the achieved results, even in the best case

**Table 3:** Results for other downstream models including.

Method	MAE	MDE	STD
Linear regression	5.16	4.12	3.83
Gaussian processes regression	5.15	4.15	4.06
Support vector machine	5.21	4.27	3.55
Multi-layered perceptron	6.61	5.46	0.03

were only around 20% better than the proposed baseline method, which is not enough to present the method as fully developed.

- Standard deviation of predictions is quite low, which supports the hypothesis of high noise presence in used dataset. To confirm the results, more experiments should be conducted with varying, but known degree of randomness in the data.
- Methods with small number of parameters, namely Otsu-based index and fractal dimension index achieve better results than those with higher number, such as 2-point correlation or vision transformer index, which agrees with the theory of statistics, in which statistical models with low number of variables are less prone to noise in the data. However, some useful features, which were not found during this analysis could exist and potentially improve the quality of the estimation. Those features could be obtained using for example frequency analysis of the image, multi-point correlation or morphological operations.

## REFERENCES

1. M. Szala, M. Szafran, W. Macek, S. Marchenko and T. Hejwowski, Abrasion Resistance of S235, S355, C45, AISI 304 and Hardox 500 Steels with Usage of Garnet, Corundum and Carborundum Abrasives, *Advances in Science and Technology Research Journal*, vol. 13, no. 4, pp. 151–161, 2019, <https://doi.org/10.12913/22998624/113244>
2. M. Szala, M. Walczak and A. Świetlicki, Effect of microstructure and hardness on cavitation erosion and dry sliding wear of HVOF deposited CoNiCrAlY, NiCoCrAlY and NiCrMoNbTa coatings, *Materials*, vol. 15, no. 1, 2022, <https://doi.org/10.3390/ma15010093>
3. P. Zhang, S. X. Li and Z. F. Zhang, General relationship between strength and hardness, *Materials Science and Engineering A*, vol. 529, no. 1, 2011, <https://doi.org/10.1016/j.msea.2011.08.061>
4. F. Khodabakhshi and A. P. Gerlich, On the correlation between indentation hardness and tensile strength in friction stir processed materials, *Materials Science and Engineering A*, vol. 789, 2020, <https://doi.org/10.1016/j.msea.2020.139682>
5. “ISO 6507–1 – Metallic materials – Vickers hardness test – Part 1: Test method,” 2018.
6. H. Tsybenko, F. Farzam, G. Dehm and S. Brinckmann, Scratch hardness at a small scale: Experimental methods and correlation to nanoindentation hardness, *Tribology International*, vol. 163, 2021, <https://doi.org/10.1016/j.triboint.2021.107168>
7. R. Thompson Martínez, G. Alvarez Bestard, A. Martins Almeida Silva and S.C. Absi Alfaro, Analysis of GMAW process with deep learning and machine learning techniques, *Journal of Manufacturing Processes*, vol. 62, 2021, <https://doi.org/10.1016/j.jmapro.2020.12.052>
8. S. Guessasma, G. Montavon and C. Coddet, Modeling of the APS plasma spray process using artificial neural networks: basis, requirements and an example, *Computational Materials Science*, vol. 29, no. 3, pp. 315–333, 2004, <https://doi.org/10.1016/j.commatsci.2003.10.007>
9. S. Krajewski and J. Nowacki, Dual-phase steels microstructure and properties consideration based on artificial intelligence techniques, *Archives of Civil and Mechanical Engineering*, vol. 14, no. 2, 2014, <https://doi.org/10.1016/j.acme.2013.10.002>
10. C. Herriott and A. D. Spear, Predicting microstructure-dependent mechanical properties in additively manufactured metals with machine- and deep-learning methods, *Computational Materials Science*, vol. 175, p. 109599, 2020, <https://doi.org/10.1016/j.commatsci.2020.109599>
11. T.M. Nunes, V. H.C. De Albuquerque, J.P. Papa, C. C. Silva, P. G. Normando, E.P. Moura and J.M.R. Tavares, Automatic microstructural characterization and classification using artificial intelligence techniques on ultrasound signals, *Expert Systems with Applications*, vol. 40, no. 8, pp. 3096–3105, 2013, <https://doi.org/10.1016/j.eswa.2012.12.025>
12. J. Jung, J.I. Yoon, H.K. Park, J.Y. Kim and H.S. Kim, An efficient machine learning approach to establish structure-property linkages, *Computational Materials Science*, vol. 156, pp. 17–25, 2019, <https://doi.org/10.1016/j.commatsci.2018.09.034>
13. J. Jung, J.I. Yoon, H.K. Park, J.Y. Kim and H.S. Kim, Bayesian approach in predicting mechanical properties of materials: Application to dual phase steels, *Materials Science and Engineering A*, vol. 743, 2019, <https://doi.org/10.1016/j.msea.2018.11.106>
14. C. Payares-Asprino, Prediction of Mechanical Properties as a Function of Welding Variables in Robotic Gas Metal Arc Welding of Duplex Stainless Steels SAF 2205 Welds Through Artificial Neural Networks, *Advances in Materials Science*, vol. 21, no. 3, 2021, <https://doi.org/10.2478/adms-2021-0019>
15. T. Trzepieciński, H.G. Lemu, Ł. Chodoła, D. Ficek and I. Szczyński, Modelling Anisotropic Phenomena of Friction of Deep-Drawing Quality Steel Sheets Using Artificial Neural Networks, *Advances in Materials Science*, vol. 21, no. 3, 2021, <https://doi.org/10.2478/adms-2021-0016>



16. N. Khatavkar, S. Swetlana and A. K. Singh, Accelerated prediction of Vickers hardness of Co and Ni-based superalloys from microstructure and composition using advanced image processing techniques and machine learning, *Acta Materialia*, vol. 196, pp. 295–303, 2020, <https://doi.org/10.1016/j.actamat.2020.06.042>
17. X. Hu, J. Li, Z. Wang and J. Wang, A microstructure-informatic strategy for Vickers hardness forecast of austenitic steels from experimental data, *Materials & Design*, vol. 201, p. 109497, 2021, <https://doi.org/10.1016/j.matdes.2021.109497>
18. R. Tibshirani, Regression Shrinkage and Selection via the Lasso, *Journal of the Royal Statistical Society. Series B (Methodological)*, vol. 58, pp. 267–288, 1996, <https://doi.org/10.1111/j.2517-6161.1996.tb02080.x>
19. P.J. Huber, Robust Regression: Asymptotics, Conjectures and Monte Carlo, *The Annals of Statistics*, vol. 1, pp. 799–821, 1973, <https://doi.org/10.1214/aos/1176342503>
20. B.B. Mandelbrot, How long is the coast of Britain? Statistical self-similarity and fractional dimension, *Science*, vol. 156, no. 3775, pp. 636–638, 1967, <http://dx.doi.org/10.1126/science.156.3775.636>
21. A. Kouzani, F. He and K. Sammut, Face image matching using fractal dimension, *Conference: Image Processing*, vol. 3, pp. 642–646, 1999, <https://doi.org/10.1109/ICIP.1999.817194>
22. H. Xu, J. Yan, N. Persson, W. Lin and H. Zha, Fractal Dimension Invariant Filtering and Its CNN-Based Implementation, *IEEE Conference on Computer Vision and Pattern Recognition (CVPR)*, pp. 3825–3833, 2017, <https://doi.org/10.1109/CVPR.2017.407>
23. Q. Duan, J. An, H. Mao, D. Liang, H. Li, S. Wang, C. Huang, Review about the Application of Fractal Theory in the Research of Packaging Materials, *Materials*, 2021; 14(4):860. <https://doi.org/10.3390/ma14040860>
24. J.P. Hyslip and L.E. Vallejo, “Fractal analysis of the roughness and size distribution of granular materials,” *Engineering Geology*, vol. 48, no. 3–4, 1997, [https://doi.org/10.1016/S0013-7952\(97\)00046-X](https://doi.org/10.1016/S0013-7952(97)00046-X)
25. J.Z. Wang, J. Ma, Q.B. Ao, H. Zhi and H.P. Tang, “Review on Fractal Analysis of Porous Metal Materials,” *Journal of Chemistry*, vol. 2015, 2015, <http://dx.doi.org/10.1155/2015/427297>
26. A. Akrami, N. Nasiri and V. Kulish, Fractal dimension analysis of Mg<sub>2</sub>Si particles of Al–15%Mg<sub>2</sub>Si composite and its relationships to mechanical properties, *Results in Materials*, vol. 7, p. 100118, 2020, <https://doi.org/10.1016/j.rinma.2020.100118>
27. W. Macek, R. Branco, M. Korpyś and T. Łagoda, Fractal dimension for bending–torsion fatigue fracture characterisation, *Measurement: Journal of the International Measurement Confederation*, vol. 184, 2021, <https://doi.org/10.1016/j.measurement.2021.109910>
28. ISO 4948–1: Steels – Classification – Part 1: Classification of steels into unalloyed and alloy steels based on chemical composition, 1982.
29. EN 10027–1: Designation systems for steels – Part 1: Steel names, 2016.
30. A.K. Krella, D.E. Zakrzewska and A. Marchewicz, The resistance of S235JR steel to cavitation erosion, *Wear*, Vols. 452–453, 2020, <https://doi.org/10.3390/ma14061456>
31. EN 10025 – European standards for structural steel. Hot rolled products of structural steels., 2019.
32. ASTM E407–07 – Standard Practice for Microetching Metals and Alloys, 2015.
33. F. Zhuang, Z. Qi, K. Duan, D. Xi, Y. Zhu, H. Zhu, H. Xiong and Q. He, A Comprehensive Survey on Transfer Learning, *Proceedings of the IEEE*, vol. 109, no. 1, 2021, <https://doi.org/10.48550/arXiv.1911.02685>
34. Nobuyuki Otsu, A Threshold Selection Method from Gray-Level Histograms, *IEEE Trans. Syst. Man Cybern*, vol. 9, no. 1, 1979, <https://doi.org/10.1109/TSMC.1979.4310076>
35. M. Tan and Q. Le, EfficientNet: Rethinking Model Scaling for Convolutional Neural Networks, *Proceedings of the 36th International Conference on Machine Learning*, vol. 97, pp. 6105–6114, 2019, <https://doi.org/10.48550/arXiv.1905.11946>
36. A. Kolesnikov, L. Beyer, X. Zhai, J. Puigcerver, J. Yung, S. Gelly and N. Houlsby, Big Transfer (BiT): General Visual Representation Learning, *European conference on computer vision*, 2019, <https://doi.org/10.48550/arXiv.1912.11370>
37. J. Devlin, M.-W. Chang, K. Lee, K. T. Google and A. I. Language, BERT: Pre-training of Deep Bidirectional Transformers for Language Understanding, *Proceedings of the 2019 Conference of the North American Chapter of the Association for Computational Linguistics: Human Language Technologies, Volume 1 (Long and Short Papers)*, Minneapolis, Minnesota, Association for Computational Linguistics, 2019, pp. 4171–4186. <https://doi.org/10.48550/arXiv.1810.04805>
38. A. Dosovitskiy, L. Beyer, A. Kolesnikov, D. Weissenborn, X. Zhai, T. Unterthiner, M. Dehghani, M. Minderer, G. Heigold, S. Gelly, J. Uszkoreit and N. Houlsby, An Image is Worth 16x16 Words: Transformers for Image Recognition at Scale, *arXiv*, 2020, <https://doi.org/10.48550/arXiv.2010.11929>
39. A. Vaswani, G. Brain, N. Shazeer, N. Parmar, J. Uszkoreit, L. Jones, A. N. Gomez, Ł. Kaiser and I. Polosukhin, Attention Is All You Need, *Conference on Neural Information Processing Systems*, 2017,

- <https://doi.org/10.48550/arXiv.1706.03762>
40. K. He, X. Zhang, S. Ren and J. Sun, Deep Residual Learning for Image Recognition, 2016 IEEE Conference on Computer Vision and Pattern Recognition (CVPR), 2016, <https://doi.org/10.48550/arXiv.1512.03385>
  41. T. Ridnik, E. Ben-Baruch, A. Noy and L. Zelnik-Manor, ImageNet-21K Pretraining for the Masses, NeurIPS 2021 Datasets and Benchmarks, 2021, <https://doi.org/10.48550/arXiv.2104.10972>
  42. J. Canny, A Computational Approach to Edge Detection, IEEE Transactions on Pattern Analysis and Machine Intelligence, vol. 6, pp. 679–698, 1986, <https://doi.org/10.1109/TPAMI.1986.4767851>
  43. E.W. Weisstein, Minkowski-Bouligand Dimension. From MathWorld—A Wolfram Web Resource., [Online]. Available: <https://mathworld.wolfram.com/Minkowski-BouligandDimension.html>.
  44. C.E. Rasmussen and C.K. I. Williams, Chapter 2: Regression, in Gaussian Processes for Machine Learning, MIT University Press Group Ltd, 2006, pp. 25–51.
  45. J.C. Platt, Probabilistic Outputs for Support Vector Machines and Comparisons to Regularized Likelihood Methods, in Advances in Large Margin Classifiers, MIT Press, 1999, pp. 61–74.
  46. C–C. Chang and C–J. Lin, LIBSVM: A library for support vector machines, ACM Transactions on Intelligent Systems and Technology, vol. 3, no. 2, 2007, <https://doi.org/10.1145/1961189.1961199>
  47. K. He, X. Zhang, S. Ren and J. Sun, Delving Deep into Rectifiers: Surpassing Human-Level Performance on ImageNet Classification, 2015 IEEE International Conference on Computer Vision (ICCV), 2015, pp. 1026–1034, <https://doi.org/10.48550/arXiv.1502.01852>